Manuscript submitted to: Volume 2, Issue 2, 79-85.

AIMS Materials Science DOI: 10.3934/matersci.2015.2.79

Received date 28 February 2015, Accepted date 29 April 2015, Published date 07 May 2015

Research article

Ohmic contacts of Au and Ag metals to n-type GdN thin films

Felicia Ullstad, Jay R. Chan, Harry Warring, Natalie Plank, Ben Ruck, Joe Trodahl and Franck Natali *

The MacDiarmid Institute for Advanced Materials and Nanotechnology, School of Chemical and Physical Sciences, Victoria University of Wellington, PO Box 600, Wellington, New Zealand

* **Correspondence:** Email: franck.natali@vuw.ac.nz; Tel: +64-4-463-5809; Fax: +64-4-463-5237.

Abstract: The rare-earth nitrides appear as attractive alternatives to dilute ferromagnetic semiconductors for spintronics device applications. Most of them combine the properties of the ferromagnet and the semiconductor, an exceedingly rare combination. In this work we have grown n-type polycrystalline semiconducting GdN layers between pre-deposited contacts made of Cr/Au and Cr/Ag. The resistivity of the GdN layers ranges from 4.4×10^{-4} Ωcm to 3.1×10^{-2} Ωcm depending on the nitrogen pressure during the growth. The electrical properties of metal/n-type GdN/metal planar junctions are investigated as a function of the temperature. The current voltage characteristics of the junctions were linear for temperatures ranging from 300 K down to 5 K, suggesting an ohmic contact between the Au or Ag metal and the n-type GdN layer.

Keywords: rare-earth nitrides; GdN; spintronics; planar heterojunctions

1. Introduction

Dilute ferromagnetic semiconductors (DMS), which are formed by a dilute concentration of magnetic atoms incorporated into a semiconducting material, are seen as the most promising materials for spintronics device applications. To date the front runners are GaN and wide band gap materials doped with transition or rare-earth metals, based on the expectation of these devices operating above room temperature [1,2]. However although there has been a lot of progress over the last decade to accomplish this task, there is still a lack of complete understanding of the ferromagnetic exchange interaction. Furthermore growth issues such as the segregation of secondary phases or generation of defects when increasing the dopant concentration must still be overcome [3,4]. On top of that, in such systems the magnetic dopants also tend to act as electronic dopants making it difficult to control independently the carrier concentration and the

magnetism [5,6]. These problems have motivated us to seek intrinsic ferromagnetic semiconductors. In this context we have shown the rare-earth nitrides (RENs) are almost unique, displaying the properties of both semiconductors and magnets, even in their purest (intrinsic) state. They offer opportunities across a broad range of optoelectronic technologies and "spintronics" applications, an emerging energy-saving branch of electronics, which utilize both the charge and the spin of electrons [7]. There is enormous potential provided by the facility for doping control of spin-aligned electrons in these intrinsic ferromagnetic semiconductors: non-volatile random access memory, reduced energy consumption, increased data processing and storage speed are only three examples of a very long list. Among the REN compounds, GdN is the most studied in part because of the maximum spin moment of 7 μ_B and zero orbital angular momentum in the half-filled 4f shell of Gd^{3+}. It has also the highest Curie temperature (Tc) of the series, reported as 70 K in most experimental studies of the past 50 years, though theoretical treatments estimate Curie temperatures that are 50% or less of the experimental values [8]. From a spintronics perspective, several groups have already succeeded in obtaining proof of concept GdN-based device structures. These include GdN-based spin-filter Josephson junctions [9,10], field effect transistor structures [11] and, most recently, the use of GdN quantum dots to enhance the efficiency of GaN tunnel junctions, [12] the development of topological insulator/GdN heterostructure devices [13] as well as magnetic tunnel junctions [14]. In part with such future device application development in mind, we have investigated planar metal/REN/metal heterojunctions composed of Au or Ag metal and polycrystalline n-type GdN. Au-based metallisations are the oldest and most widely used ohmic contacts due to the relatively low electric contact resistance and excellent resistance against corrosion. For comparison we have use an Au-free metal contact made of Ag. In order to gain insight into the details of electronic nature and charge transport across these interfaces, current-voltage measurements at different temperatures from 300 K down to 5 K have been performed.

2. Materials and Method

The films used here were grown on pre-deposited contacts on sapphire substrates. Prior to the GdN growth, two sets of contacts Cr(3 nm)/Au(50 nm) and Cr(3 nm)/Ag(50 nm) were made by evaporating Cr and Au and Cr and Ag respectively onto the sapphire substrate through a shadow mask. The sapphire substrate was cut into 15 × 20 mm rectangles before contact deposition. Cr was deposited first to improve the adhesion of Au and Ag onto the sapphire substrate. The metal deposition rate was kept around 0.5 $Å s^{-1}$. The shadow mask produced a few sets of six contact pad pairs with a spacing of between 30 and 100 μm. Figure 1 shows the typical pattern of the pre-deposited contacts on the substrate. After deposition the sets of contacts were sonicated in acetone at room temperature for 10 minutes to remove kapton tape residues from the mounting process during contact deposition. No thermal annealing on the pre-deposited contacts was performed. The pre-deposited contacts were then introduced into an ultra-high vacuum system (base pressure < 5×10^{-8} Torr), and the GdN layers were deposited at ambient temperature between the pre-deposited contacts. The pre-deposited contacts were partially protected by a shadow mask in order to leave part of the contact uncoated for making electrical contact. The GdN growth rate was maintained at 2 $Å s^{-1}$ controlled by the Gd evaporation rate and monitored throughout by a piezoelectric quartz crystal monitor, in an atmosphere of nitrogen ranging from 2.4 to 3.6×10^{-5} mbar. Nitrogen purity of 99.999% was used with content of carbon dioxide less than 1 ppm,

hydrocarbons (as methane) less than 1 ppm, oxygen less than 2 ppm, moisture less than 2 ppm. The Gd was thermally evaporated using an electron gun on a solid Gd target (purity: 99.9%). The GdN films grown were ~150 nm thick and to prevent their decomposition in air they were capped with a ~50 nm thick GaN layer. X-ray reflectometry performed on GdN layers grown on sapphire substrates without pre-deposited contacts and under similar conditions yielded a thickness of 150 ± 5 nm, consistent with the crystal monitor. The crystalline structure was assessed by X-ray diffraction (XRD). A single polycrystalline GdN phase is observed in the XRD 2θ-scans (Figure 2), as expected for the growth of an fcc rock-salt structure on a (0001) wurtzite surface [15,16]. In addition to the (0001) sapphire peak we observe only (111) and (222) reflections of GdN. No evidence of impurity phases, such as Gd_xO_y or pure Gd, is found. The out of plane lattice constants of the GdN films are about 5.01 Å, close to the bulk value of 4.998 Å reported in the literature and suggesting that all films are fully relaxed [6]. The XRD linewidths yield crystal coherence lengths in the sample plane of typically 10 to 15 nm.

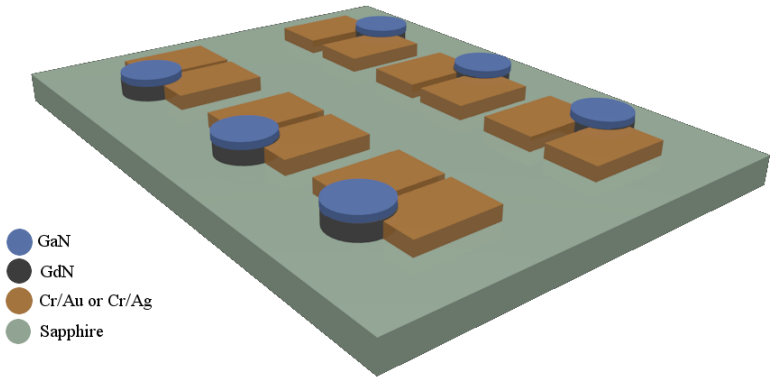

Figure 1. Schematic illustration of the planar metal/GdN/metal junctions prepared for the contact-resistance measurement.

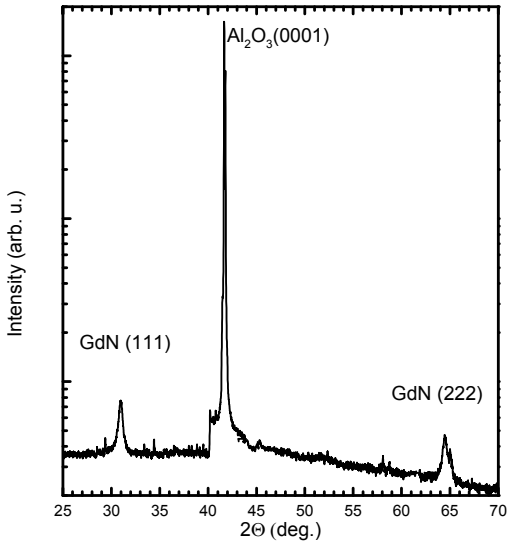

Figure 2. 2Θ-scan XRD scan of a polycrystalline GdN films grown at room temperature on a sapphire substrate.

3. Results and Discussion

We turn to the electrical properties by showing first the temperature dependent resistivity for GdN films without pre-deposited contacts measured in the van der Pauw geometry (Figure 3). The room temperature resistivity is rather low for a semiconductor. This indicates that the low nitrogen pressure during the growth results in an n-type layer with a high concentration of free electrons due to nitrogen vacancies (V_N), as both we and others have concluded previously [17]. The film with the highest resistivity was grown in a nitrogen partial pressure of about 3.5×10^{-5} mbar compared to 2.4×10^{-5} mbar for the film with the lowest resistivity signaling that a reduced concentration of V_N in the film grown with a larger nitrogen pressure. The resistivity of the GdN layers in this study ranges from 4.4×10^{-4} Ωcm to 3.1×10^{-2} Ωcm depending on the nitrogen pressure during the growth. In each case the n-type GdN films show a semiconductor-like resistivity behaviour and the peak in the resistivity coincides with the ferromagnetic ordering temperature (Tc~50–70K) as previously reported [8,15,16,18].

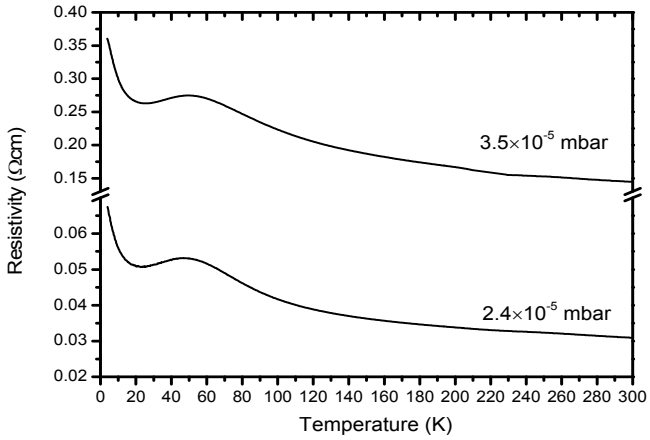

Figure 3 Temperature dependent resistivity for samples grown under different nitrogen pressures. In each case the peak in the resistivity coincides with the ferromagnetic ordering temperature.

We now focus on the electrical properties of Au/n-type GdN/Au junctions made of GdN layers with resistivity of 4.4×10^{-4} Ωcm (sample A) and 3.1×10^{-2} Ωcm (sample B), respectively. The temperature dependent resistance of the Au/n-type GdN/Au junction-sample A (figure 4) suggests it is dominated by the Au contact, with a positive temperature coefficient of resistance (TCR) characteristic of a metal. Indeed a similar GdN film grown in the same condition without pre-deposited contacts shows a semiconductor-like temperature dependence of the resistance similar to the samples displayed in Figure 3, leading us to conclude that the TCR of the resistance versus temperature of sample A is due to the Au contacts. However note that a resistivity peak at the 50 K suggests also a significant contribution of the GdN layer in the total resistance. Interestingly sample B (Figure 4), which is more resistive, shows a GdN-like resistance behavior suggesting that the resistance of the planar junction is completely dominated by the resistance of the GdN layer. The current-voltage (I-V) characteristics at 290 K, 60 K and 5 K of sample A and sample B are displayed in Figure 5. The curves are linear at all temperatures, from 290 K down to 5 K, suggesting an ohmic

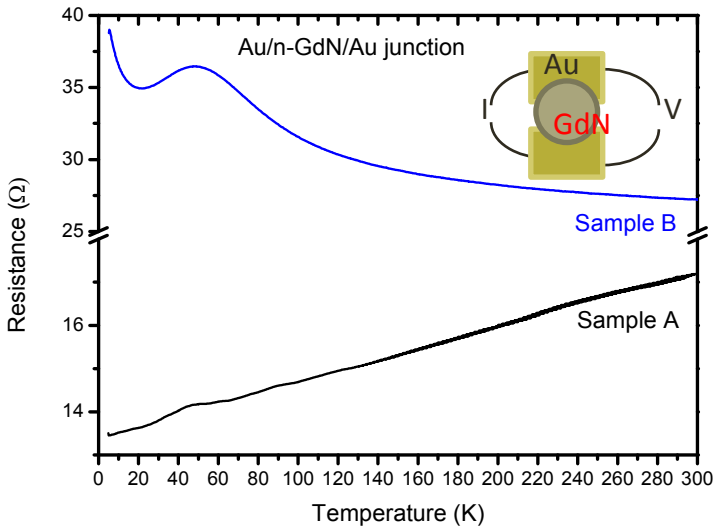

Figure 4. The temperature dependent resistance of: (a) the Au/n-type GdN/Au junction-sample A and (b) the Au/n-type GdN/Au junction-sample B. For both samples the distance between the contacts is 40 µm. The schematic illustration shows the geometry used for the measurement.

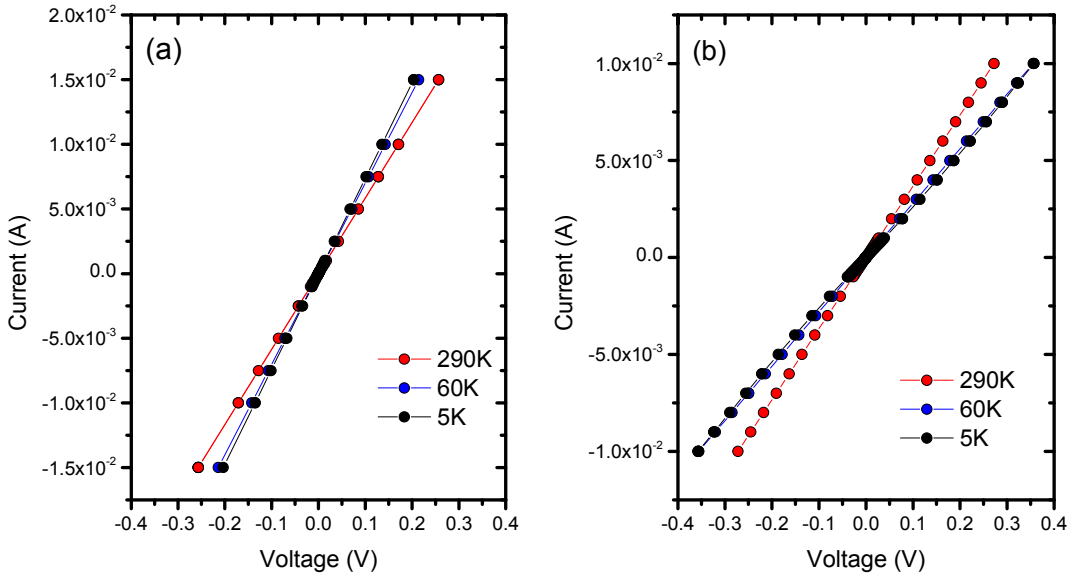

Figure 5. Current-voltage characteristics of (a) sample A and (b) sample B at different temperatures.

behavior. Note that all the junctions in the studied range show ohmic behavior irrespective of their contact separation. We have also investigated the electrical properties of an Ag/n-type GdN/Ag junction-sample C, made of a GdN layer with resistivity identical to sample B, 3.1×10^{-2} Ωcm. The resistance of the junction is dominated by the GdN layer resistance in the same way as sample B (not shown). The I-V characteristics also show a linear behavior at all temperatures, characteristic of an Ag/n-type ohmic contact. It worth pointing out that the resistivity of the polycrystalline GdN layers in this study is comparable with the resistivity of a wide range of epitaxial GdN thin films that would

be used in most of the REN-based spintronics devices [19]. This makes Au and Ag promising metal candidates for the fabrication of ohmic contacts on not only n-type GdN but any semiconducting rare earth nitrides.

4. Conclusion

We have fabricated and studied the electrical properties of metal/n-type GdN/metal planar junctions. The GdN layers are grown at room temperature between either pre-deposited Au or Ag contacts, and show an n-type conductivity, primarily due to doping by nitrogen vacancies. The current voltage characteristics of the junctions were linear for temperatures ranging from 290 K down to 5 K, suggesting an ohmic contact between the Au and Ag metal and the n-type GdN layer.

Acknowledgments

We acknowledge funding from the Marsden Fund (Grant No. 13-VUW-1309) and the MacDiarmid Institute for Advanced Materials and Nanotechnology, funded by the New Zealand Centres of Research Excellence Fund. We also wish to thank Dr. Olly Pantoja for X ray reflectivity measurements that support this paper.

Conflict of Interest

The author declares no conflicts of interest in this paper.

References

1. Dhar S, Brandt O, Ramsteiner M, et al. (2005) Colossal Magnetic Moment of Gd in GaN. *Phys Rev Lett* 94: 037205.
2. Murmu PP, Kennedy J, Williams GVM, et al. (2012) Observation of magnetism, low resistivity, and magnetoresistance in thenear-surface region of Gd implanted ZnO. *Appl Phys Lett* 101: 082408.
3. Chen ZT, Wang L, Yang XL, et al. (2010) Mechanism of ultrahigh Mn concentration in epitaxially grown wurtzite $Ga_{1-x}Mn_xN$. *Appl Phys Lett* 97: 222108.
4. Navarro-Quezada A, Stefanowicz W, Li T, et al. (2010) Embedded magnetic phases in (Ga,Fe)N: Key role of growth temperature. *Phys Rev B* 81: 205206.
5. Dobrowolska M, Tivakornsasithorn K, Liu X, et al. (2012) Controlling the Curie temperature in (Ga,Mn)As through location of the Fermi level within the impurity band. *Nature Mater* 11: 444–449.
6. Natali F, Ruck BJ, Plank NOV, et al. (2013) Rare-earth mononitrides. *Prog Mater Sci* 58: 1316–1360.
7. Mitra C, Lambrecht WRL (2008) Magnetic exchange interactions in the gadolinium pnictides from first principles. *Phys Rev B* 78: 134421.
8. Natali F, Ruck BJ, Trodahl HJ, et al. (2013) Role of magnetic polarons in ferromagnetic GdN. *Phys Rev B* 87: 035202.

9. Senapati K, Blamire MG, Barber ZH (2011) Spin-filter Josephson junctions. *Nature Mater* 10: 849–852.
10. Blamire MG, Pal A, Barber ZH, et al. (2013) Spin filter superconducting tunnel junctions. *Proc SPIE*, Spintronics V 8461.
11. Warring H, Ruck BJ, Trodahl HJ, et al. (2013) Electric field and photo-excited control of the carrier concentration in GdN. *Appl Phys Lett* 102: 132409.
12. Krishnamoorthy S, Kent T, Yang J, et al. (2013) GdN Nanoisland-Based GaN Tunnel Junctions. *Nano Lett* 13: 2570–2575.
13. Kandala A, Richardella A, Rench DW, et al. (2013) Growth and characterization of hybrid insulating ferromagnet-topological insulator heterostructure devices. *Appl Phys Lett* 103: 202409.
14. Warring H, Trodahl HJ, Plank NOV, et al. (2015) Magnetic tunnel junctions based on the intrinsic ferromagnetic semiconductor GdN. Appl. Phys. Lett. [submitted].
15. Scarpulla MA, Gallinat CS, Mack S, et al. (2009) GdN (111) heteroepitaxy on GaN (0001) by N_2 plasma and NH_3 molecular beam epitaxy. *J Cryst Growth* 311: 1239–1244.
16. Natali F, Plank NOV, Galipaud J, et al. (2010) Epitaxial growth of GdN on silicon substrate using an AlN buffer layer. *J Cryst Growth* 24: 3583.
17. Natali F, Ludbrook B, Galipaud J, et al. (2012) Epitaxial growth and properties of GdN, EuN and SmN thin films. *Phys Status Solidi C* 9: 605.
18. Granville S, Ruck BJ, Budde F, et al. (2006) Semiconducting ground state of GdN thin films. *Phys Rev B* 73: 35335.
19. Lee C-M, Warring H, Vézian S, et al. (2015) Highly resistive epitaxial Mg-doped GdN thin films. *Appl Phys Lett* 106: 022401